COMMUNICATION

# L-proline, a resolution agent able to target both enantiomers of mandelic acid: an exciting case of stoichiometry controlled chiral resolution.

Received 00th January 20xx,
Accepted 00th January 20xx

DOI: 10.1039/x0xx00000x

Fuli Zhou,[a] Laurent Collard [a], Koen Robeyns[a], Tom Leyssens*[a] and Oleksii Shemchuk[a]

**We present a thought-provoking development in chiral resolution. Using a resolving agent of a given handedness, L-proline, we show that both R- and S-enantiomers of mandelic acid can be resolved from a racemic mixture simply by varying the stoichiometry. We are the first to report this specific feature, achieved by the existence of stoichiometrically diverse cocrystal systems between R- and S-mandelic acid and L-proline.**

Cocrystals have become one of the principal targets in the quest for materials with novel or improved supramolecular properties. Research into the design and application of cocrystals has grown in recent years since they are capable of tuning the physicochemical properties of materials and hence allow widening potential applications.[1-8] In addition, cocrystals have a great advantage over salts since they, in principle, can be formed for all compounds.

Chiral resolution, the process allowing separation of enantiomers, is one of the fields where cocrystallization has shown its potential. Initially, cocrystallization was introduced as an alternative to "classical" – chiral resolution via diastereomeric salt formation.[9] This latter approach uses the difference in solubility between two diastereomers to selectively crystallize the less soluble diastereomer. Unlike salt-forming systems, for which diastereomeric pair formation appears to be the general rule, cocrystal systems more frequently behave enantiospecifically, with a chiral resolving agent only forming a cocrystal with one of the two enantiomers of the target molecule. An experimental cocrystal screen combined with an extensive CSD search showed that for about 85% of cocrystal systems an enantiospecific rather than a diastereomeric character was encountered.[10] Chiral resolution via enantiospecific cocrystal formation has been successfully employed in a number of cases.[11-14] During the last couple of years, achiral cocrystallizing agents have also shown their use in the context of resolution,[15-17] with cocrystallization mainly being used to transform a racemic compound into a conglomerate. This latter system can then be used for resolution through preferential crystallization.[18,19] We, recently, extended this approach, showing the potential to simultaneously resolve two racemic compounds through preferential cocrystallization.[18]

Here, we further expand the toolbox of cocrystal resolution processes, by showing how the cocrystal stoichiometry can be used to specifically target either of the enantiomers of a racemate using the same resolution agent (so of the same handedness). Specifically, we show how either of the enantiomers of RS-mandelic acid can be resolved merely by adapting the amount of L-proline[†] (scheme 1). This astonishing feature is explained by the existence of thermodynamically stable and stoichiometrically diverse cocrystals with both enantiomers of mandelic acid - R-MAN·L-PRO (**RL**) and S-MAN·L-$PRO_2$ (**$SL_2$**). To the best of our knowledge, this is the first example of a salt or cocrystal system where a resolving agent of a given handedness can be used to target either one of the two enantiomers of a racemate.

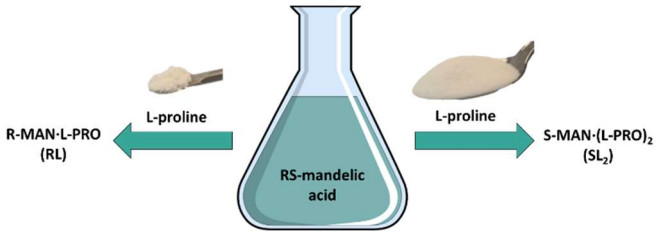


**Scheme 1.** By adapting the amount of L-proline either the R-, or S-enantiomer of mandelic acid can be resolved.

The obtained cocrystal reaction outcome between L-proline and mandelic acid depends both on the handedness of mandelic acid, as well as the overall proline/mandelic acid ratio as shown in scheme 2, compiled from grinding experiments (see Fig. ESI-

[a] Institute of Condensed Matter and Nanosciences, Université catholique de Louvain, 1 Place Louis Pasteur, B-1348 Louvain-La-Neuve, Belgium Address here.
[b] *Email:* tom.leyssens@ulcouvain.be

Electronic Supplementary Information (ESI) available: [details of any supplementary information available should be included here]. See DOI: 10.1039/x0xx00000x

1-6). Long grinding periods, and cross seeding during grinding experiments were performed to assure a thermodynamic outcome.

$$R + L \longrightarrow RL \quad (1)$$
$$S + L \longrightarrow SL \quad (2)$$
$$RS + L \longrightarrow RL + SL \quad (3)$$
$$R + 2L \longrightarrow RL + L \quad (4)$$
$$S + 2L \longrightarrow SL_2 \quad (5)$$
$$RS + 2L \longrightarrow RL + SL_2 \quad (6)$$

**Scheme 2**. Cocrystallization outcome at the solid state when grinding racemic mandelic acid or its enantiomers with one or two equivalents of L-proline.

Using equimolar amounts of L-proline and either of the mandelic acid enantiomers, a diastereomeric pair of cocrystals - R-MAN·L-PRO + S-MAN·L-PRO (**RL** + **SL**) is obtained (eqs. 1 and 2). Racemic mandelic acid is also dismantled into this pair using one equivalent of L-proline (eq. 3). As stoichiometrically diverse cocrystals are often encountered working with amino acids,[19-23] we also performed grinding experiments using various amounts of proline. The use of 2 equivalents of L-proline indeed led to a stoichiometrically diverse cocrystal system with S-mandelic acid forming the 1:2 S-MAN·(L-PRO)$_2$ (**SL$_2$**) cocrystal (eq.5). Interestingly, the 1:2 diastereomeric cocrystal involving R-mandelic acid does not form (eq. 4). This can be explained by the fact that cocrystal formation reactions are often characterized by free energies of formation ( $\Delta G°$) of a couple of kcal·mol$^{-1}$.[24-31] Changes in the structure of a coformer (such as a change in stereochemistry) can therefore have a substantial impact on the success of cocrystal formation. This would explain why a stoichiometrically diverse system is obtained working with S-mandelic acid, while for R-mandelic acid only the 1:1 cocrystal exists. As a consequence, the use of 2 equivalents of L-proline dismantles the racemate to yield a mixture of **RL** and **SL$_2$** cocrystals (eq.6).

All of the above-mentioned cocrystals were analyzed by single crystal analysis, with simulated patterns overlapping with the experimental ones (Figs ESI-4-6). **SL** (Fig. 1a) crystallizes in the monoclinic $P2_1$ space group with two molecules of S-mandelic acid and two molecules of L-proline in the asymmetric unit (Z'=2) (for detailed structural information on this and the other structures see table ESI-1). In turn, its diastereomeric counterpart, **RL** (Fig. 1b), crystallizes in the orthorhombic $P2_12_12_1$ space group with one R-mandelic acid and one L-proline molecule in the asymmetric unit cell.

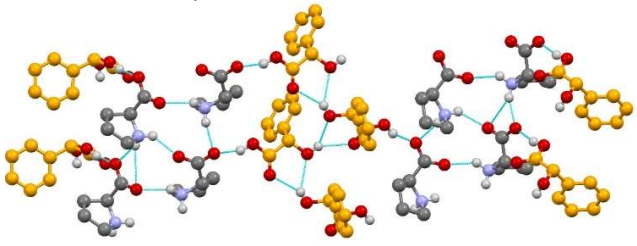

a)

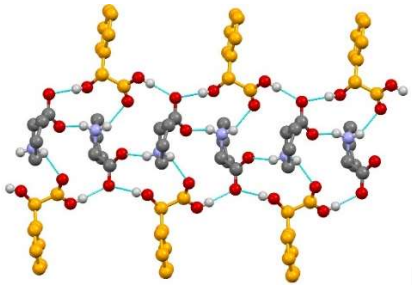

b)

**Fig. 1**. Hydrogen bonding interactions in crystalline **SL** (a) and **RL** (b). $H_{CH}$ are omitted for clarity and carbons of mandelic acid are orange.

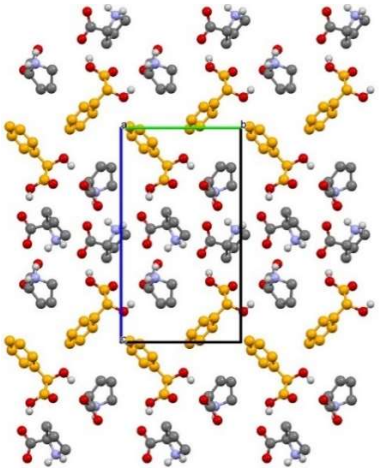

**Fig. 2**. Crystal packing of **SL$_2$**. $H_{CH}$ are omitted for clarity and carbons of S-mandelic acid are orange.

The stoichiometrically diverse cocrystal S-MAN·(L-PRO)$_2$ (**SL$_2$**) crystallizes in the monoclinic $P2_1$ space group with one S-mandelic acid and two L-proline molecules in the asymmetric unit (Fig. 2).

To get a clear overview of the thermodynamics behind the various combinations, the solid-state landscape between both enantiomers of mandelic acid and L-proline was investigated by constructing a ternary phase diagram from grinding experiments. This diagram (Fig. 3) shows all thermodynamically stable situations when combining various ratios of the starting components. These diagrams are also of importance for future resolution development, as they highlight those solid forms (or combinations thereof) for which stable suspensions can be identified. In our case, stable suspensions containing a single solid form can be obtained for **RS**-, **S**- and, **R**-mandelic acid, **L**-proline, as well as for the **RL**, **SL** and **SL$_2$** cocrystals. A suspension of two different solid forms is limited to the combinations shown in bold green (e.g. **RL** + **L** or **RL** + **SL**, … with a suspension of e.g. **L** + **RS** being thermodynamically unstable). Finally, suspensions of three different solid forms can be obtained for the combinations shown in red (e.g. an **RL** + **SL** + **RS** suspension is stable whereas an **R** + **S** + **L** suspension is not). The exact nature of the solid forms obtained in suspension depends on the amount and nature of solvent added and requires the construction of a quaternary phase diagram.

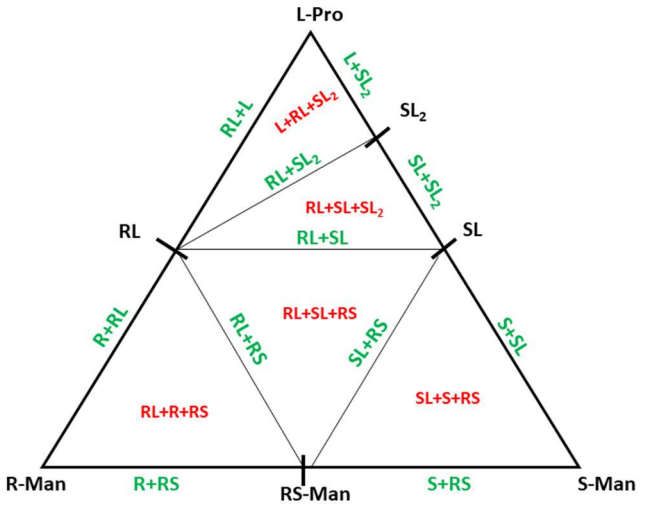


**Fig. 3.** Ternary solid-state phase. A single pure solid is noted in black/ single point; a mixture of 2 phases in green / line; a mixture of 3 phases in red / zone (triangle).

Based on the fact that a diastereomeric system is obtained for the 1:1 cocrystal stoichiometry and that the 1:2 cocrystal only forms with S-mandelic acid, we envisioned resolving both R- and S-mandelic acid from a racemate, merely varying the amount of L-proline added. This would be the first resolution process where a resolving agent of a given handedness (L-proline) is used to resolve both enantiomers (R- and S-mandelic acid) starting from a racemic solution, in contrast to classical diastereomeric resolution, where a change in chirality of resolving agent is required to target the compound of opposite chirality.

Our methodology requires the **RL** diastereomer to be more stable than the **SL** diastereomer, and an appropriate solvent to be identified for which the **RL** and **$SL_2$** cocrystals can be obtained in suspension without the presence of solid forms containing the opposite enantiomer.

A preliminary solvent screen (see table ESI-3) starting from a racemic mandelic acid solution, and using various amounts of L-proline, led to suspensions of **RL** as sole solid form or in combination with **RS-man** and/or **$SL_2$**. The **SL** solid form was never observed indicating the **RL** diastereomer to be thermodynamically favored over the **SL** diastereomer, satisfying the first of the requirements mentioned above.

Ethanol was then chosen for further development, as the full transformation of racemic mandelic acid in cocrystal solid forms was always observed (no signals of RS-mandelic acid in the resulting XRPD pattern), and a suspension containing only the **RL** solid form was obtained during the initial screen using a 2:1 mandelic acid/proline ratio.‡

To identify conditions allowing resolution of both mandelic acid enantiomers using L-proline, we investigated the isoplethal (fixed R/S ratio for mandelic acid) ternary phase diagram between RS-mandelic acid, L-proline and ethanol (Fig. 4). This diagram should be seen as a cut in the complete quaternary phase diagram between ethanol, L-proline, and R- and S-mandelic acid. An initial screen (Fig. 4a) showed RS-mandelic acid to be much more soluble compared to L-proline, explaining why less solvent was used when screening the right side of the diagram.

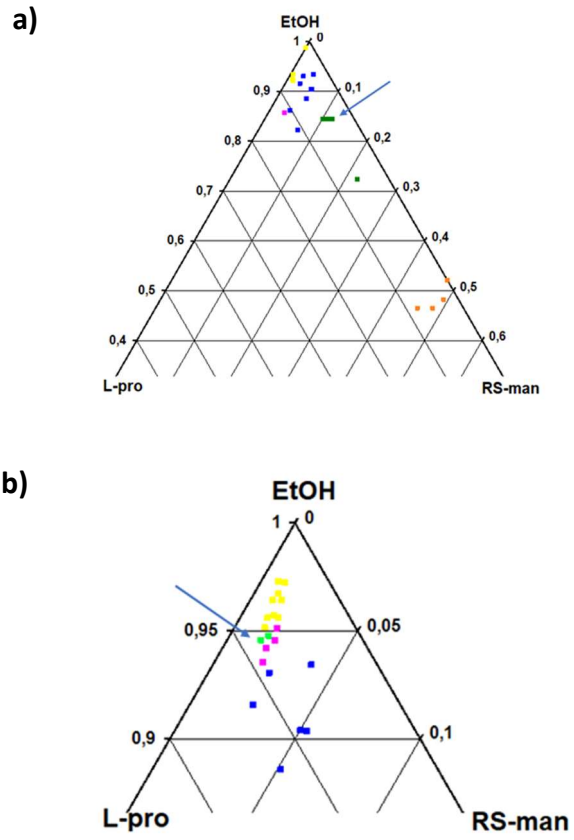


**Fig. 4.** Isoplethal ternary diagram (mole fraction) between RS-mandelic acid, L-proline and ethanol. (a) initial screen (Table ESI-4), (b) zoom on the top left part of the diagram (Table ESI-5). Solids in suspension are RS-man (orange), **RL** (dark green), **RL** + **$SL_2$** (blue), **RL**+**$SL_2$**+L-Pro (pink), L-Pro (yellow), and **$SL_2$** + L-Pro (bright green).

Using increasing amounts of proline, a large zone is identified for which the **RL** cocrystal (dark green dots) is the only stable form in suspension. This zone corresponds to those conditions that can be used to effectively resolve R-mandelic acid from a racemate. Further increasing the amount of L-proline, we identified a large zone where a mixture of two cocrystals – **RL** and **$SL_2$** was thermodynamically stable in suspension (blue dots). Analysis of the XRPD patterns of the obtained solids, showed a clear tendency towards an increased amount of **$SL_2$** when using higher quantities of L-proline, whereas the amount of **RL** decreased (Fig. ESI-10). This incited us to look in more detail at the top left part of the diagram to identify conditions under which **$SL_2$** can be obtained in suspension without the presence of the **RL** form (Fig. 4b and table ESI-5).

Unsurprisingly, this part of the diagram shows the use of high quantities of L-proline will lead to conditions where this compound is the only stable form in suspension (yellow dots),

with low amounts of solvent leading to a suspension (pink dots) containing both **$SL_2$** and **RL** cocrystals (so both enantiomers of mandelic acid). Interestingly enough, a zone was identified where the **$SL_2$** cocrystal is obtained in combination with L-proline (bright green dots). Under these conditions, the S-enantiomer of mandelic acid is the only enantiomer found in a solid form, and hence these conditions can be effectively used to resolve the S-enantiomer from a racemate, fulfilling the second requirement mentioned above.

We were, therefore, able to identify conditions allowing resolution both of R- and S-mandelic acid starting from a racemate, by merely varying the amount of L-proline. This is, to the best of our knowledge, the first such reported system and highlights how cocrystallization can be used to add new tools to the resolution toolbox.

We scaled up the resolution for both enantiomers (conditions used are highlighted by the blue arrows in Fig. 4 and described in the SI), and subsequently separated L-proline from the obtained cocrystal as explained in the supporting information. This led to the recovery of R-mandelic acid with an *ee*>99% (Fig. SI-9), and of S-mandelic acid with an *ee*>96% (Fig. ESI-13).

This work is the first to introduce a stoichiometry-controlled resolution process, using a chiral resolution agent of a given handedness to resolve both enantiomers of a racemate by merely varying the stoichiometry of the system. Both R- and S-mandelic acid can be resolved from solution, using the appropriate amount of L-proline. This specific feature can be achieved through the fact that a diastereomeric pair of 1:1 cocrystals exists, whereas the 1:2 cocrystal only occurs for the S-enantiomer. Scaling up the process, we were able to recover both R- and S-mandelic acid from a racemate with an ee>99% and ee>96% respectively.

This unique system highlights the immense potential cocrystallization has in chiral resolution and is the first system for which it is shown that a mere change in stoichiometry allows targeting either one of the two enantiomers of a racemic solution.

## Conflicts of interest

There are no conflicts to declare.

## Acknowledgements

FZ would like to thank the China Scholarship Council (CSC) for financial support. OS is a FNRS postdoctoral researcher. The research is funded by FNRS PDR grant (T.0149.19 – T.262.20).

## Notes and references

* For clarity different nomenclature was used for both compounds, keeping D-/L-prefixes for the amino acid proline and R-/S-prefixes for mandelic acid.

* This selection was merely based on initial results and does not imply another solvent cannot lead to even better results.

1. J. Wouters and L. Quéré, *Pharmaceutical salts and co-crystals*, Royal Society of Chemistry, 2011.
2. E. Nauha and M. Nissinen, *J. Mol. Struct.*, 2011, **1006**, 566-569.
3. J. W. Steed, *Trends Pharmacol Sci*, 2013, **34**, 185-193.
4. C. A. Gunawardana and C. B. Aakeroy, *Chem. Commun.*, 2018, **54**, 14047-14060.
5. F. Liang, N. Wang, X. Liu, Z. Lin and Y. Wu, *Chem. Commun.*, 2019, **55**, 6257-6260.
6. P. A. Julien, L. S. Germann, H. M. Titi, M. Etter, R. E. Dinnebier, L. Sharma, J. Baltrusaitis and T. Friscic, *Chem Sci*, 2020, **11**, 2350-2355.
7. X. Meng, K. Kang, Y. Liu, J. Tang, X. Jiang, W. Yin, Z. Lin and M. Xia, *Cryst. Growth Des.*, 2020, **20**, 7588-7592.
8. Y. Liu, A. Li, S. Xu, W. Xu, Y. Liu, W. Tian and B. Xu, *Angew. Chem. Int. Ed.*, 2020, **59**, 15098-15103.
9. D. Kozma, *CRC handbook of optical resolutions via diastereomeric salt formation*, Crc Press, 2001.
10. G. Springuel, K. Robeyns, B. Norberg, J. Wouters and T. Leyssens, *Cryst. Growth Des.*, 2014, **14**, 3996-4004.
11. G. Springuel and T. Leyssens, *Cryst. Growth Des.*, 2012, **12**, 3374-3378.
12. O. Sánchez-Guadarrama, F. Mendoza-Navarro, A. Cedillo-Cruz, H. Jung-Cook, J. I. Arenas-García, A. Delgado-Díaz, H. Morales-Rojas and H. Höpfl, *Cryst. Growth Des.*, 2015, **16**, 307-314.
13. B. Harmsen and T. Leyssens, *Cryst. Growth Des.*, 2017, **18**, 441-448.
14. L. He, Z. Liang, G. Yu, X. Li, X. Chen, Z. Zhou and Z. Ren, *Cryst. Growth Des.*, 2018, **18**, 5008-5020.
15. L. C. Harfouche, C. Brandel, Y. Cartigny, S. Petit and G. Coquerel, *Chem. Eng. Technol.*, 2020, **43**, 1093-1098.
16. X. Buol, C. Caro Garrido, K. Robeyns, N. Tumanov, J. Wouters and T. Leyssens, *Cryst. Growth Des.*, 2020, **20**, 7979-7988.
17. O. Shemchuk, F. Grepioni, T. Leyssens and D. Braga, *Isr. J. Chem.*, 2021, **61**, 563-572.
18. F. Zhou, O. Shemchuk, M. D. Charpentier, L. Collard, J. H. Ter Horst and T. Leyssens, *Angew. Chem. Int. Ed.*, 2021, **60**, 20264-20268.
19. A. Tilborg, G. Springuel, B. Norberg, J. Wouters and T. Leyssens, *CrystEngComm*, 2013, **15**.
20. A. Tilborg, T. Leyssens, B. Norberg and J. Wouters, *Cryst. Growth Des.*, 2013, **13**, 2373-2389.
21. A. Tilborg, B. Norberg and J. Wouters, *Eur. J. Med. Chem.*, 2014, **74**, 411-426.
22. N. Tumanova, N. Tumanov, F. Fischer, F. Morelle, V. Ban, K. Robeyns, Y. Filinchuk, J. Wouters, F. Emmerling and T. Leyssens, *CrystEngComm*, 2018, **20**, 7308-7321.
23. N. Tumanova, N. Tumanov, K. Robeyns, F. Fischer, L. Fusaro, F. Morelle, V. Ban, G. Hautier, Y. Filinchuk, J. Wouters, T. Leyssens and F. Emmerling, *Cryst. Growth Des.*, 2018, **18**, 954-961.
24. M. Habgood, M. A. Deij, J. Mazurek, S. L. Price and J. H. ter Horst, *Cryst. Growth Des.*, 2009, **10**, 903-912.
25. P. G. Karamertzanis, A. V. Kazantsev, N. Issa, G. W. A. Welch, C. S. Adjiman, C. C. Pantelides and S. L. Price, *J. Chem. Theory Comput.*, 2009, **5**, 1432-1448.
26. M. Habgood and S. L. Price, *Cryst. Growth Des.*, 2010, **10**, 3263-3272.
27. S. Mohamed, D. A. Tocher and S. L. Price, *Int. J. Pharm.*, 2011, **418**, 187-198.
28. M. Habgood, *Cryst. Growth Des.*, 2013, **13**, 4549-4558.
29. G. L. Perlovich, *CrystEngComm*, 2015, **17**, 7019-7028.
30. G. L. Perlovich, *CrystEngComm*, 2017, **19**, 2870-2883.
31. D. Ahuja, M. Svärd, M. Lusi and Å. C. Rasmuson, *CrystEngComm*, 2020, **22**, 3463-3473.

 